2025 IEEE/SICE International Symposium on System Integration (SII)
January 21-24, 2025, Munich, Germany

Stiffness Measurement and Modeling of Robot Arm Consisting of Single Geared Joint and Link Made of Different Materials

Naoyuki Takesue[1], Kazuma Sugihara[1], Gen Endo[2], Yuta Tsukamoto[2], and Takeshi Takaki[3]

***Abstract*— The aim of this study is to establish a lightweight construction method for robot elements using metal and plastic materials in order to achieve energy saving in industrial robots. However, in general, weight reduction reduces stiffness, which in turn reduces the performance required for industrial robots. This paper presents an experimental setup and models to investigate the effects of link stiffness and joint stiffness on overall stiffness, and demonstrates the validity of the models through experiments. Then, experiments with different link materials were conducted and the results were compared. The influence of the fastening method and the fastening torque of the link on the stiffness of the entire system was clarified.**

I. Introduction

The demand for industrial robots continues to grow every year, and this trend is expected to continue in the future[1]. In addition, efforts to achieve the United Nations Sustainable Development Goals (SDGs) and carbon neutrality have gained momentum in recent years. In this context, energy conservation of industrial robots is desirable. The power consumption of industrial robots depends largely on their weight. Therefore, weight reduction of industrial robots is expected to contribute to energy conservation.

One way to reduce robot weight is to replace traditional metal materials with new lightweight materials such as composites and resins. However, weight reduction generally reduces stiffness, which tends to lower the high-speed, high-position control performance required for industrial robots. At present, the evaluation of the use of new materials as robot parts is not sufficient, and further study is needed.

Therefore, this study aims to establish a construction method for lightweight industrial robots using metal and resin materials for energy saving. The previous work focused on the link and joint. Four types of links (made of A5052, POM, Onyx, and Onyx with carbon fiber) were mounted on a single-axis robot, and the stiffness models of the joint and link were verified[2]. Although some studies have modeled a robot joint gear[3], [4], [5], [6], this study presented a stiffness model of the entire system consisting of the joint gear and the link.

In this paper, a measurement experiment system was reconstructed and modeled to more accurately predict the influence of the deformation of each fastener and component on the stiffness of the entire system, and to compare the amount of deformation caused by each material in detail. By identifying the fasteners and components that have a large impact on the stiffness of the entire system and comparing them with each material, it is expected that it will be possible to study effective countermeasures, such as optimizing the shape of joint parts and developing fastening methods[7].

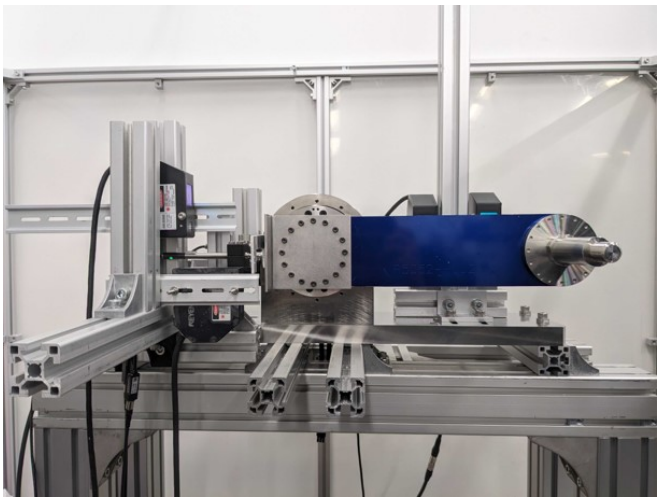

Fig. 1: Experimental apparatus for stiffness measurement

This paper is organized as follows. Section 2 describes the configuration of the robot arm experimental apparatus and its stiffness model. Section 3 describes the axial stiffness experiments of the robot arm. Section 4 describes further experiments on the stiffness characteristics in the rotational direction. Section 5 presents the experimental results of the influence of fastening conditions on the stiffness. Finally, section 6 summarizes the paper.

II. Experimental apparatus configuration and stiffness model

The experimental apparatus used to evaluate the stiffness is shown in Fig. 1. A list of the materials used for the link components to be evaluated is also shown in Fig. 2. The experimental apparatus was a single-axis articulated robotic arm consisting of a servo actuator (Harmonic Drive Systems, SHA32M101SG-B12B200-16S17bA-C) equipped with a wave gearing device (commercially known as Harmonic Drive®) and a link (different materials).

A. Configuration

The output flange is attached to the servo actuator with 16 M5 bolts (grade 12.9), and the link is attached to the output flange with 16 M4 bolts (grade 12.9) via an L-shaped mounting plate, as shown in Fig 3. The flange part was

[1]Naoyuki Takesue and Kazuma Sugihara are with Tokyo Metropolitan University, Hino-shi, Tokyo, Japan. [2]Gen Endo and Yuta Tsukamoto are with Tokyo Institute of Technology, Japan. [1]Takeshi Takaki is with Hiroshima University, Japan.

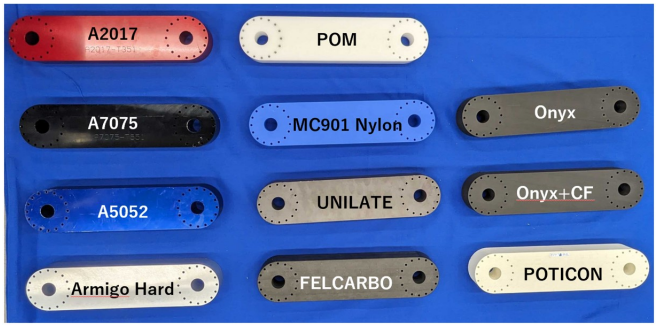

Fig. 2: List of links

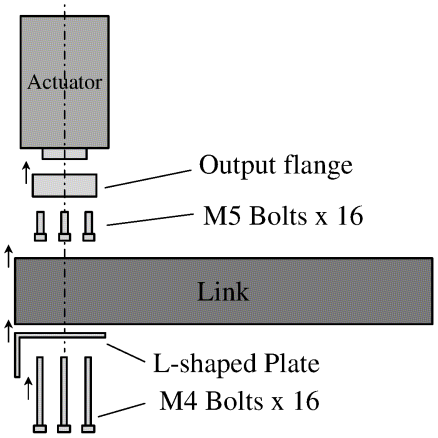

Fig. 3: Joint and link mounting part

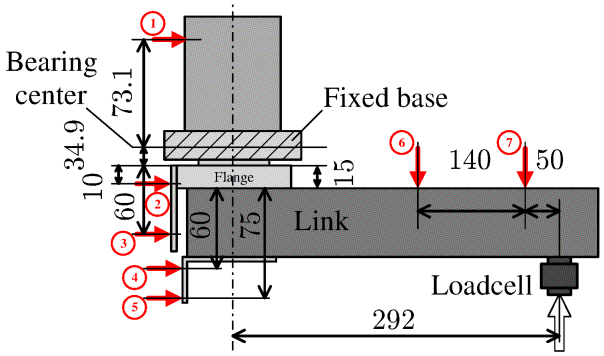

Fig. 4: Measurement positions when axial load is applied

tightened with a torque wrench to a torque of 3.0 N·m and the link mounting part was tightened to a torque of 1.5 N·m or 3.6N·m (in section 5), using the T series as the tightening torques for the various mounting parts. After each fastener part was tightened, the displacement of each displacement sensor was reset to 0 and set as the reference point.

In the experiment, a force of about 100 N was applied in the axial and rotational directions at the end of the links via a load cell (Figs. 4 and 5). To obtain the deformation of the robot arm, laser sensors (Keyence, LK-G35 and LK-G85) and contact-type digital sensors (Keyence, GT2-P12KL) were used for the axial experiment at the points ① to ⑦ in Fig. 4. For the rotational experiment, rotary

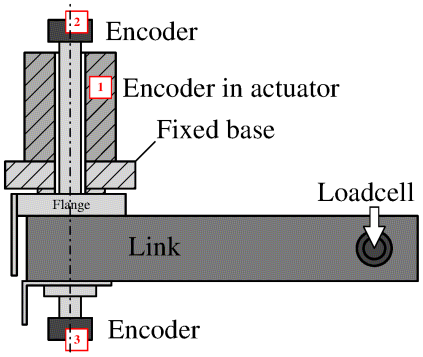

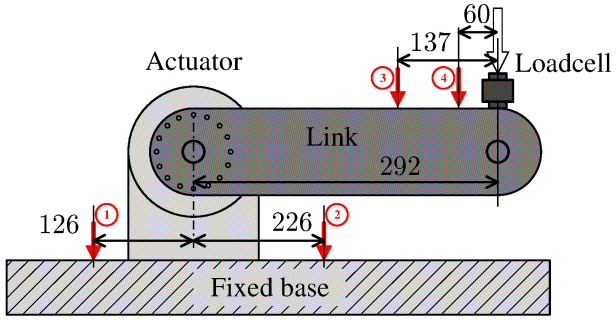

Fig. 5: Measurement positions when rotational load is applied

encoders (Harmonic Drive Systems, built-in encoder and Microtech Laboratory, MEH-59-12960PST256E) were used at the points of [1] to [3] in Fig. 5, and the laser sensors were used at the points ① to ④ in Fig. 5. To reduce the influence of variation in the measurement data, the displacement was measured 10 times with a load applied. In addition, a brake was applied to hold the motor shaft, and the experiment was conducted with the motor rotation fixed in the servo-locked state.

B. Modeling

The models for which the main elastic deformations have been studied in Figs. 4 and 5 are shown in Figs. 6 and 7, respectively. When an external force is applied to the link tip of this model as indicated by the white arrow in the figures, each part is considered to be deformed as shown in Figs. 8 and 9. Therefore, by measuring the displacements (angles) at the actuator case, actuator flange, link root and link tip, for example, as shown in Fig. 4, the equivalent moment stiffness of each part can be obtained.

The stiffness of entire system is expressed as follows:

$$K_{\mathrm{Ent},*} = \frac{K_{*0}K_{*1}K_{*2}K_{*3}}{K_{*0}K_{*1}K_{*2}+K_{*0}K_{*1}K_{*3} \\ +K_{*0}K_{*2}K_{*3}+K_{*1}K_{*2}K_{*3}} \quad (1)$$

where $*$ is a or r, depending on whether the direction of the applied force is axial or rotational. As can be seen from this equation, since the stiffness of an component affects the overall stiffness, it can be said that simply increasing the stiffness of an component does not increase the overall stiffness very much. In other words, increasing the stiffness

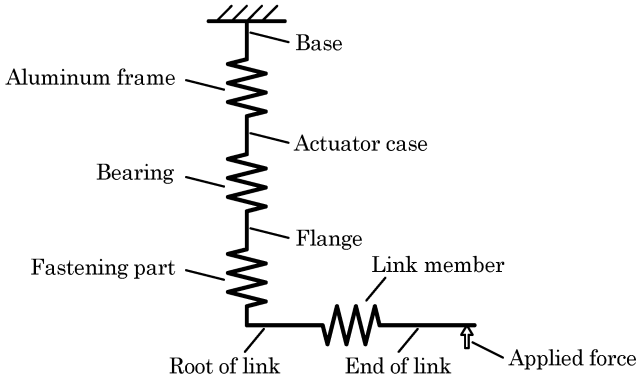

Fig. 6: Stiffness model in axial direction

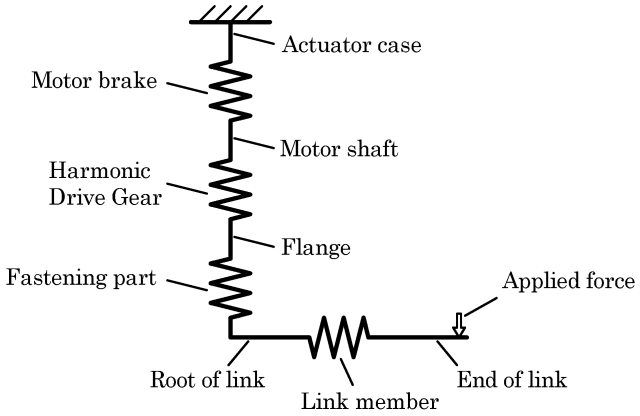

Fig. 7: Stiffness model in rotational direction

of the least stiff component will have a positive effect on the overall stiffness.

III. Stiffness Measurement Experiment in Axial Direction

To demonstrate the validity of the deformation model of the experimental apparatus as shown in Fig. 8 when a force of about 100 N (a moment of about 29.2 N·m) is applied in the axial direction, verification experiments were conducted using A5052 link material. As in the considered deformation model, the displacement angle increased toward the tip of the system, and the measurement results were consistent with the deformation model in which deformations were accumulated at each part of the experimental apparatus.

Next, based on the results of the validation experiments, we conducted axial stiffness measurement experiments using different link materials, and obtained the stiffness of each component of the experimental apparatus. The material differences were not significant for K_{a0} and K_{a1}. The K_{a0} and K_{a1} were calculated as follows:

$$K_{a0} = 7.00 \times 10^5 \text{ [N·m/rad]} \quad (2)$$

$$K_{a1} = 9.86 \times 10^5 \text{ [N·m/rad]} \quad (3)$$

The stiffness K_{a1} is related to the bearing in the actuator. Since the moment stiffness in the actuator manual[8] is 100×10^4 N·m/rad, it is almost identical.

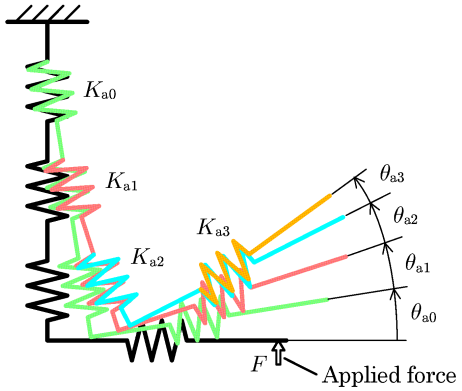

Fig. 8: Deformation model in axial direction

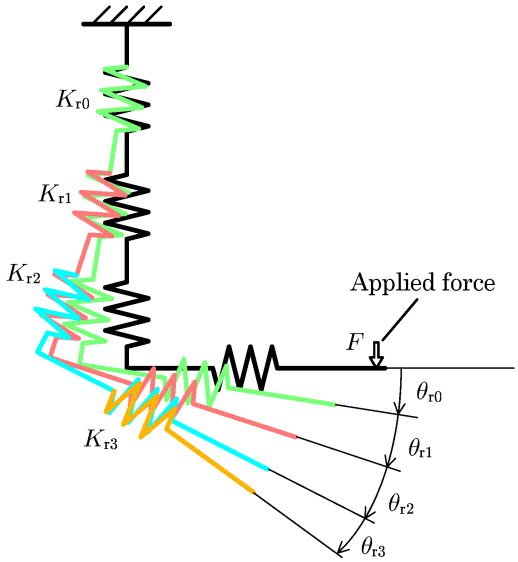

Fig. 9: Deformation model in rotational direction

The material differences were visible for K_{a2}, and the differences were even more pronounced for K_{a3}. Table I shows K_{a2}, K_{a3} and $K_{\text{Ent},a}$ calculated based on the deformation model considered when force is applied in the axial direction.

In evaluating the stiffness for each link material, the stiffness using resin materials and 3D-printed linkage parts was inferior to that of the system using conventional metal linkage parts, confirming that the range of application is limited. On the other hand, it was also found that developing the internal structure of the link parts, such as mixing continuous fibers[9] in Onyx[10], was effective in terms of stiffness.

IV. Stiffness Measurement Experiment in Rotational Direction

A validation experiment was conducted using A5052 link material to demonstrate the validity of the deformation model of the experimental apparatus as shown in Fig. 9 when a force is applied in the rotational direction. Measurement results

TABLE I: Moment stiffness (axial direction) at fastening part and link part with fastening torque of 1.5 N·m

	Material	Moment stiffness [N·m/rad]		
		K_{a2}	K_{a3}	$K_{\mathrm{Ent},a}$
Al	Armigo Hard	1.13×10^6	7.26×10^5	2.13×10^5
	A7075-T631	1.04×10^6	6.16×10^5	1.97×10^5
	A2017-T351	9.30×10^5	5.88×10^5	1.94×10^5
	A5052-H112	1.05×10^6	6.24×10^5	2.00×10^5
Plastic	FELCARBO	3.87×10^5	1.38×10^5	8.14×10^4
	UNILATE	2.19×10^5	9.17×10^4	5.57×10^4
	POM	1.31×10^5	2.48×10^4	1.98×10^4
	MC901 Nylon	1.35×10^5	2.95×10^4	2.29×10^4
3DP	Onyx+CF	6.83×10^4	1.30×10^4	1.06×10^4
	POTICON	6.11×10^4	1.18×10^4	9.66×10^3
	Onyx	1.96×10^4	3.08×10^3	2.64×10^3

TABLE II: Moment stiffness (rotational direction) at link fastening part and link part with fastening torque of 1.5 N·m

	Material	Moment stiffness [N·m/rad]		
		K_{r2}	K_{r3}	$K_{\mathrm{Ent},r}$
Al	Armigo Hard	9.30×10^5	2.89×10^6	1.42×10^5
	A7075-T631	6.82×10^5	2.35×10^6	1.34×10^5
	A2017-T351	4.43×10^5	2.30×10^6	1.22×10^5
	A5052-H112	8.49×10^5	2.68×10^6	1.42×10^5
Plastic	FELCARBO	3.08×10^5	6.64×10^5	9.56×10^4
	UNILATE	2.85×10^5	3.88×10^5	8.66×10^4
	POM	2.58×10^5	9.18×10^4	4.89×10^4
	MC901 Nylon	2.60×10^5	1.15×10^5	5.54×10^4
3DP	Onyx+CF	8.71×10^4	5.40×10^4	2.81×10^4
	POTICON	8.61×10^4	4.24×10^4	2.45×10^4
	Onyx	3.96×10^4	1.17×10^4	8.58×10^3

consistent with the deformation model were obtained in the rotational direction.

Then, based on the results of the validation experiment, the stiffness measurement experiments in the rotational direction were conducted with different link materials, and the stiffness of each component of the experimental apparatus was obtained for each link material.

K_{r0} and K_{r1} are independent of the material of the link and were obtained as follows:

$$K_{r0} = 4.87 \times 10^7 \text{ [N·m/rad]} \quad (4)$$

$$K_{r1} = 1.83 \times 10^5 \text{ [N·m/rad]} \quad (5)$$

In the actuator specifications[8], the rotational stiffness is 6.7 to 12×10^4 N·m/rad depending on the applied torque. The resulting K_{r1} is relatively higher than the specifications.

Although no significant difference was observed between the link materials for K_{r0} and K_{r1}, the differences appeared for K_{r2} and K_{r3}. Table II shows K_{r2}, K_{r3} and $K_{\mathrm{Ent},r}$ calculated based on the deformation model considered when force is applied in the rotational direction.

When evaluating the stiffness in the rotational direction for each link material, the stiffness using the resin materials and 3D-printed link parts was also inferior to that of the device using conventional metal link parts in the rotational stiffness measurement experiment. The same tendency as in the axial stiffness measurement experiment was also observed in the problems and improvement methods for incorporating the resin materials into the device.

TABLE III: Moment stiffness (axial direction) with fastening torque of 3.6 N·m

Material	Moment stiffness [N·m/rad]		
	K_{a2}	K_{a3}	$K_{\mathrm{Ent},a}$
A5052-H112	1.93×10^6	6.24×10^5	2.16×10^5
FELCARBO	6.00×10^5	1.48×10^5	9.22×10^4
Onyx	2.20×10^4	3.09×10^3	2.69×10^3

TABLE IV: Moment stiffness (rotational direction) with fastening torque of 3.6 N·m

Material	Moment stiffness [N·m/rad]		
	K_{r2}	K_{r3}	$K_{\mathrm{Ent},r}$
A5052-H112	1.07×10^6	2.70×10^6	1.47×10^5
FELCARBO	4.23×10^5	6.77×10^5	1.03×10^5
Onyx	4.32×10^4	1.22×10^4	9.01×10^3

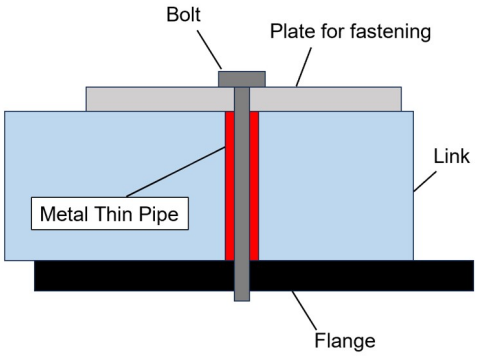

Fig. 10: Fastening method by Endo et al.[7]

V. Effect of Fastening Conditions on Stiffness

A. Effect of fastening torque

The effect of the fastening torque of the link on the stiffness is investigated. A5052, FELCARBO, and Onyx were used as representative materials for aluminum alloy, plastic (CFRP), and 3D printer materials, respectively. The stiffness obtained from the experimental results is shown in Tables III and IV when the link was fixed with a fastening torque of 3.6 N·m. It was confirmed that the stiffness K_{a2}, K_{r2} of the link fastener was improved for all link materials in both directions of the experiment.

On the other hand, the improvement in the stiffness of the 3D-printed link (Onyx) by increasing the fastening torque of the link was small compared to other link materials. Therefore, it was confirmed that the stiffness of the entire robot cannot be greatly improved by increasing the fastening torque of the link alone, and therefore it is necessary to devise the fastening method and the internal structure of the link parts.

B. Effects of fastening method

Next, to solve the problem of fastening parts made of 3D printed plastic parts, the bolt fastening method proposed by Endo et al.[7] was incorporated into the experimental apparatus, and the effect on stiffness was determined experimentally. The configuration of the fastener is shown in Fig 10. The stiffness of K_{a2}, K_{a3}, $K_{\mathrm{Ent},a}$ and K_{r2}, K_{r3}, $K_{\mathrm{Ent},r}$

TABLE V: Moment stiffness (axial direction) with fastening method by Endo et al.[7]

Material	Fastening torque [N·m]	Moment stiffness [N·m/rad]		
		K_{a2}	K_{a3}	$K_{\mathrm{Ent},a}$
Onyx	1.5	4.11×10^4	7.53×10^3	6.27×10^3
Onyx	3.6	5.99×10^4	7.79×10^3	6.78×10^3

TABLE VI: Moment stiffness (rotational direction) with fastening method by Endo et al.[7]

Material	Fastening torque [N·m]	Moment stiffness [N·m/rad]		
		K_{r2}	K_{r3}	$K_{\mathrm{Ent},r}$
Onyx	1.5	6.19×10^4	1.31×10^4	1.02×10^4
Onyx	3.6	9.11×10^4	1.38×10^4	1.13×10^4

obtained from the stiffness measurement experiments in both directions are shown in Tables V and VI. In the stiffness measurement experiments in both directions, the stiffness K_{a2}, K_{r2} was increased, and when the fastening torque was increased, the stiffness K_{a2}, K_{r2} was further increased, contributing to the improvement of the overall stiffness.

On the other hand, the stiffness K_{a3}, K_{r3} of the link part is still not sufficient, and it was confirmed that further improvement of the link fastening method and the internal structure of the link parts is necessary for the 3D printed parts.

VI. Conclusions

In this study, we constructed and modeled an experimental apparatus for measuring the axial and rotational stiffness of a robot arm consisting of links and single geared joint, and investigated the effects of each component of the experimental apparatus on the stiffness of the entire apparatus by changing the link materials and fastening conditions. It was found that the stiffness of the link fasteners and link components has a significant effect on the stiffness of the entire system, and that the improvement methods include the use of different fastening conditions and internal structures of the link components.

Future plans include adding evaluation materials, comparing link fastening methods, comparing the effect of the internal structure of link parts on the stiffness of the entire system, and adding robot performance evaluation.

Acknowledgement

This research was subsidized by the New Energy and Industrial Technology Development Organization (NEDO) under project JPNP20016. This paper is an achievement of joint research with and is jointly owned copyrighted material of the ROBOT Industrial Basic Technology Collaborative Innovation Partnership.

We thank Prof. Yusuke Ohta (Chiba Institute of Technology) for his valuable comments and discussion.

References

[1] (2024, Aug.) International Federation of Robotics, "Global industrial robot sales doubled over the past five years". [Online]. Available: https://ifr.org/ifr-press-releases/news/global-industrial-robot-sales-doubled-over-the-past-five-years

[2] Naoyuki Takesue, Yuri Ode: Stiffness Model of Single-Geared Joint with 3D-Printed Link in Robot Arm, IEEE/SICE Int. Symp. on System Integrations, pp.525-530, 2023.

[3] Claire Dumas, Stéphane Caro, Cherif Mehdi, Sébastien Garnier, Benoît Furet: Joint Stiffness Identification of Industrial Serial Robots, Robotica, Cambridge University Press, pp.1-20, 2011.

[4] Zhifeng Liu, Jingjing Xu, Qiang Cheng, Yongsheng Zhao and Yanhu Pei: Rotation-joint stiffness modeling for industrial robots considering contacts, Advances in Mechanical Engineering, Vol.10, No.8, pp.1-13, 2018.

[5] Kun Yang, Wenyu Yang, Guangdong Cheng, Bingrong Lu: A new methodology for joint stiffness identification of heavy duty industrial robots with the counterbalancing system, Robotics and Computer Integrated Manufacturing, Vol.53, pp.58-71, 2018.

[6] Peng Xu, Xiling Yao, Shibo Liu, Hao Wang, Kui Liu, A. Senthil Kumar, Wen Feng Lu, Guijun Bi: Stiffness modeling of an industrial robot with a gravity compensator considering link weights, Mechanism and Machine Theory, Vol.161, 104331, 2021.

[7] Gen Endo, Yuta Tsukamoto, Hiroyuki Nabae, and Takeshi Takaki: Proposal of a Fastening Method for Deformable Plastic Parts and Rigid Metal Parts , IEEE/SICE Int. Symp. on System Integrations, pp.503-508, 2023.

[8] (2024, Aug.) Harmonic Drive Systems Inc., "AC Servo Actuator SHA SG/CG series manual", [Online]. Available: https://www.harmonicdrive.net/_hd/content/catalogs/pdf/csg-gh-catalog.pdf

[9] (2024, Aug.) Markforged, Carbon Fiber. [Online]. Available: https://markforged.com/materials/continuous-fibers/continuous-carbon-fiber

[10] (2024, Aug.) Markforged, Onyx. [Online]. Available: https://markforged.com/materials/plastics/onyx